



LAWRENCE
LIVERMORE
NATIONAL
LABORATORY

Downstream Intensification Effects Associated with CO₂ Laser Mitigation of Fused Silica

M. J. Matthews, I. L. Bass, G. M. Guss, C. C.
Widmayer, F. L. Ravizza

November 6, 2007

SPIE - Boulder Damage Symposium
Boulder, CO, United States
September 24, 2007 through September 26, 2007

Disclaimer

This document was prepared as an account of work sponsored by an agency of the United States government. Neither the United States government nor Lawrence Livermore National Security, LLC, nor any of their employees makes any warranty, expressed or implied, or assumes any legal liability or responsibility for the accuracy, completeness, or usefulness of any information, apparatus, product, or process disclosed, or represents that its use would not infringe privately owned rights. Reference herein to any specific commercial product, process, or service by trade name, trademark, manufacturer, or otherwise does not necessarily constitute or imply its endorsement, recommendation, or favoring by the United States government or Lawrence Livermore National Security, LLC. The views and opinions of authors expressed herein do not necessarily state or reflect those of the United States government or Lawrence Livermore National Security, LLC, and shall not be used for advertising or product endorsement purposes.

Downstream Intensification Effects Associated with CO₂ Laser Mitigation of Fused Silica

Manyalibo J. Matthews, Isaac L. Bass, Gabriel M. Guss, Clay C. Widmayer and Frank L. Ravizza

Lawrence Livermore National Laboratory, 7000 East Avenue, Livermore, CA 94550

ABSTRACT

Mitigation of 351nm laser-induced damage sites on fused silica exit surfaces by selective CO₂ treatment has been shown to effectively arrest the exponential growth responsible for limiting the lifetime of optics in high-fluence laser systems. However, the perturbation to the optical surface profile following the mitigation process introduces phase contrast to the beam, causing some amount of downstream intensification with the potential to damage downstream optics. Control of the laser treatment process and measurement of the associated phase modulation is essential to preventing downstream ‘fratricide’ in damage-mitigated optical systems. In this work we present measurements of the surface morphology, intensification patterns and damage associated with various CO₂ mitigation treatments on fused silica surfaces. Specifically, two components of intensification pattern, one on-axis and another off-axis can lead to damage of downstream optics and are related to rims around the ablation pit left from the mitigation process. It is shown that control of the rim structure around the edge of typical mitigation sites is crucial in preventing damage to downstream optics.

Keywords: laser-induced damage, fused silica, laser damage mitigation

INTRODUCTION

The operation of large aperture, high fluence laser systems such as the National Ignition Facility, depend on an effective remanufacturing or ‘recycling’ strategy to maximize the lifetime of high cost optics prone to damage [1-4]. In particular, the fused silica optics used as focusing elements are generally quite thick (~4cm), and must be produced from high-quality, inclusion-free SiO₂, making these elements relatively expensive and of highest interest in terms of damage repair and recycling.

Although some amount of damage due to transport and handling of the optics (e.g. scratches, contamination) can contribute to the damage, it is primarily the laser induced damage that drives the rate of recycling. Moreover, unlike other fused silica elements in systems like NIF, SiO₂ focusing lenses are traditionally placed after converting 1 ω light to 2 and 3 ω light, which imposes a lower relative (exit surface) damage threshold on these lenses versus other silica elements. Once a damage site has initiated, it is not only the optical loss (scattering) and added modulation (contrast) imposed on the beam that limits performance, but more the threat of macroscopic fracture through the bulk if the damage is allowed to grow from multiple shots [5]. Fortunately, earlier detection of damage initiation using in-situ imaging diagnostics has been shown to be effective at identifying damage initiations and estimating their size in order to remove optics for recycling.

In the ideal recycling scenario, once the optic is removed and ready for refurbishment, each damage site would be treated by a process that would return the optic to exactly its original condition, so that its performance in the laser system is indistinguishable from a pristine optic. However, such an operation is currently impractical given the high-grade finish that accompanies a new optic, and alternatives involving some acceptable modification of the damaged region must be pursued. Recently, CO₂ laser damage mitigation has been shown to repair and arrest the growth of damage sites created from 351nm pulses [1-4]. Because the region of the optical surface that was once damaged then becomes transformed into a region different from the original pristine material, limits must be placed on this transformation in terms of laser

operation. First and foremost, the transformed region must not contain any features of the original damage site which were prone to damage growth. Second, while the original fractured material that was associated with damage growth may have effectively been removed or made harmless, the transformation itself may introduce material that essentially behaves the same way, i.e. damages immediately upon 3ω laser exposure. Such is the case for redeposited material that is removed from damage mitigation processes. Care must therefore be taken to ensure this material is re-fused with the surface or is swept away. And while local treatment of the silica surface may leave that region of the surface free from damage initiators – or even enhance the damage threshold – non-local effects such as stress can lead to a shortened lifespan of the optic due to rapid crack growth upon nearby damage initiations. Finally, given that laser light is not only incident on the region but passes through it, the third important constraint to be placed on the transformation of the damaged surface is that of phase perturbation to the optical system. Departure from the original flat surface began with the damage event itself, and generally, the transformation of the damage region introduced by mitigation involves further departure. Specifically, the resulting surface morphology associated with the mitigation transformation must not lead to the focusing of light on other downstream optics above their respective damage thresholds.

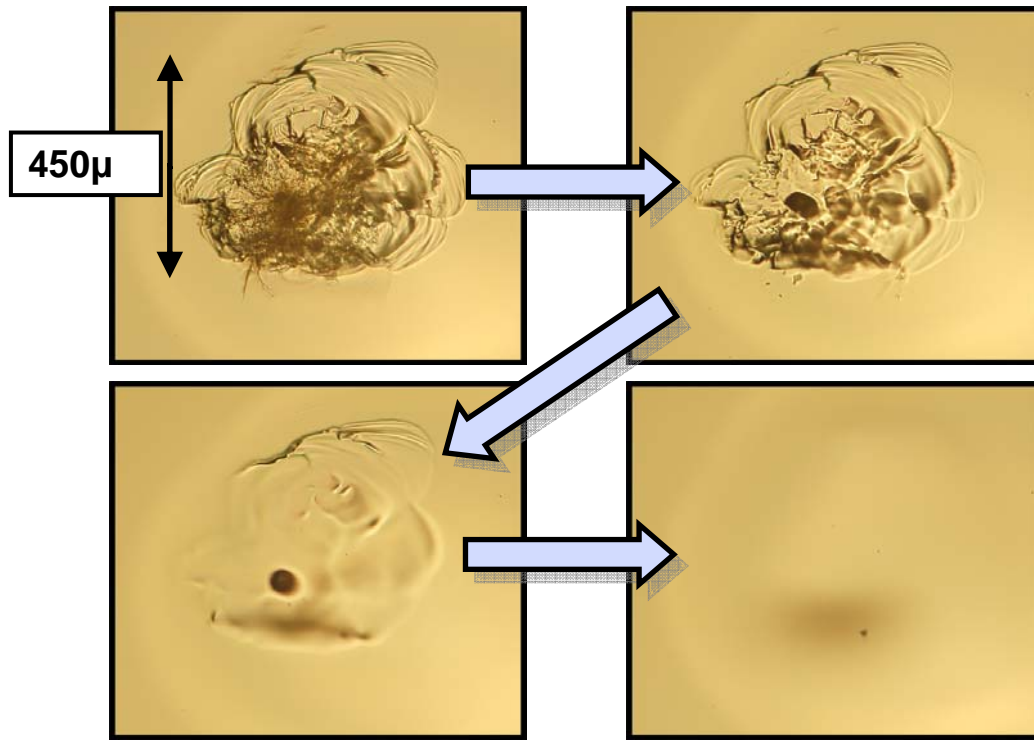


Figure 1: Optical micrographs showing the transformation of laser-induced damage from a fractured crater to a smooth, relatively featureless mitigation site. The site shown above was mitigated using $4.6\ \mu\text{m}$ laser exposures [3], which penetrate deeper into the bulk, but generally produce similar final morphologies.

In this paper, we discuss the important features associated with the surface morphology introduced by the mitigation of fused silica surface damage, the associated phase perturbations they produce and subsequent damage to optics placed downstream from the sites. While the smooth crater, the dominant feature of the mitigation site, introduces some amount of light focusing hazard, it is shown that the outer rim of this crater, associated with evaporation and material flow of the glass, causes the more intense downstream modulation. By controlling the rim structure of the mitigation sites, it is shown through propagation calculations and direct downstream damage testing that an effective solution to this problem can be accomplished.

EXPERIMENTAL DETAILS

The samples used in this study, both for creation of the CO₂ mitigation sites and for downstream intensification damage testing were 50.8mm diameter, 10mm thick Corning 7980 fused silica rounds. Samples were lightly etched in buffered HF (BOE) then precision cleaned using FL-70 detergent and a 10% NaOH solution. Mitigation sites on pristine starting material were created using single shot exposures or raster scanning a CO₂ laser with axial irradiances ranging from 0 to 16 kW/cm² and exposures ranging from 5ms to 1s. A complete description of the mitigation process can be found in Ref. 6. Surface morphologies were studied using a STIL contactless profilometer, which is based on focusing a broadband source through an achromatic objective and spectrally resolving the back reflections using a monochromator and diode array. The axial and lateral resolution of the STIL profilometer was ~0.5μm and ~1μm respectively. Damage testing was performed at the Optical Sciences Laser Laboratory at LLNL, using weakly focusing, 3ns Gaussian, 351nm pulses with a flat top spatial profile roughly 10mm in diameter.

SURFACE MORPHOLOGIES OF CO₂ IRRADIATED SITES

Figure 2 illustrates the general cross sectional surface figure produced by CO₂ laser irradiation, showing that, while the fracture associated with the damage can be removed by evaporation and remelting [4, 7], the resulting shape is characterized by a crater region and a surrounding raised rim. This rim is formed from mass movement of silica at high temperatures from the low viscosity central region outwards, and can be several microns high under conditions used to mitigate surface damage (see Table I).



Figure 2: Drawing depicting the transformation of a damage site into a mitigation crater, indicating the removal of material via evaporation in the center (over an area roughly equal to the $1/e^2$ of the laser spot), and a formation of a rim caused by mass movement along the surface.

In order to study the effect of different morphologies on downstream intensification, four CO₂ treated sites corresponding to four different types of mitigation were studied. The surface morphology of each is shown in Fig. 3. Site A was produced by a single, fixed 35ms exposure at ~16kW/cm² axial irradiance, and can be considered a reasonable treatment for small damage sites <100μm. Sites B-D, were produced under similar conditions, but using galvanometer mirrors to raster the beam in a spiral pattern across the surface. Site D differed from sites A-C, in that a final ‘dimpled’ patterning was performed in the rim region. The resulting shapes, as parameterized in Fig. 4, are shown in Table I.

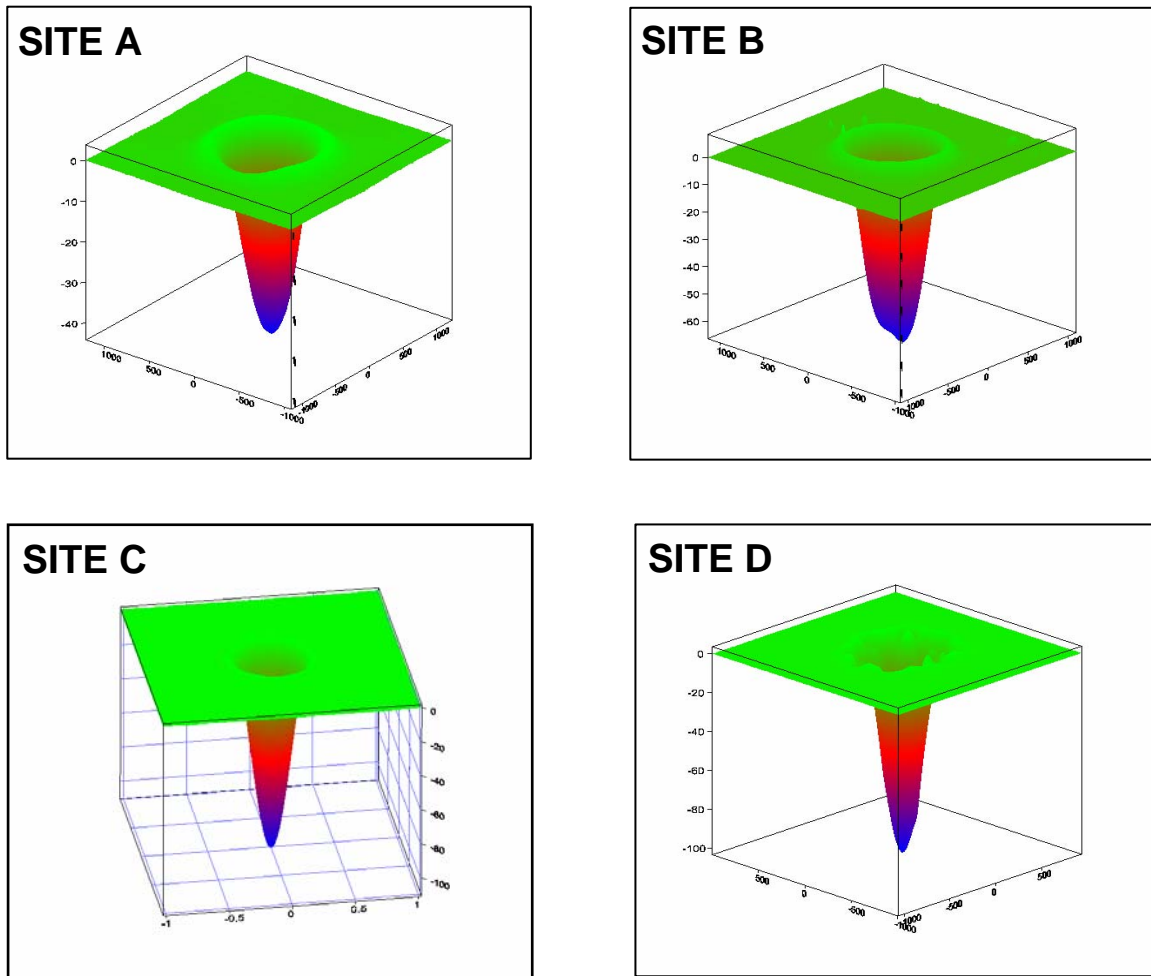


Figure 3: Surface morphologies of the four sites studied: Single exposure site produced using a 35ms pulse (Site A), 1s exposures around a 300 and 500 μm spiral pattern, (Sites B and C respectively), and a rim-reduced or 'dimpled' version of Site C where 5ms exposures were used to evaporate away portions of the raised rim (x and y dimensions are in mm, z dimension is in microns).

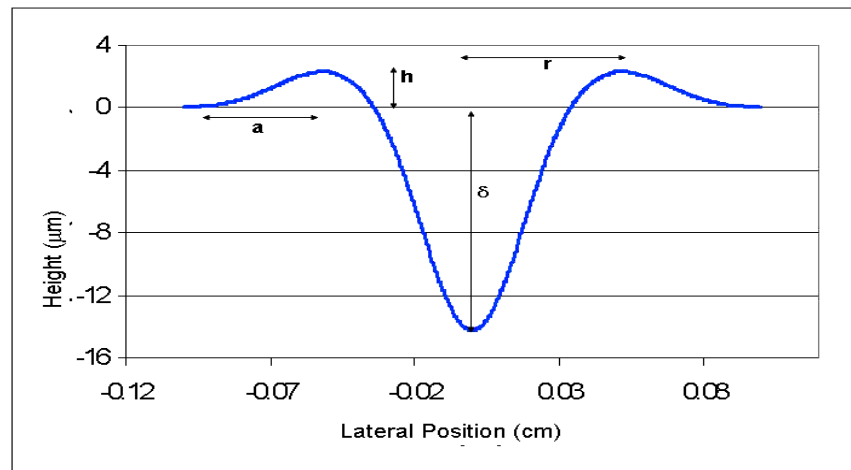


Figure 4: Parameterization of the general surface profile associated with CO_2 exposures on fused silica.

Table I: Surface morphology parameters for the sites studied.

| | a (μm) | r (μm) | h (μm) | δ (μm) | Z (mm) |
|--------|---------------------|---------------------|---------------------|----------------------------|----------------|
| SITE A | 202 ± 12 | 135 ± 5 | 2.8 ± 0.6 | 43 ± 0.7 | 19.5 ± 4.4 |
| SITE B | 113 ± 17 | 226 ± 4 | 4.6 ± 0.6 | 63 ± 1.6 | 11.1 ± 2.2 |
| SITE C | 120 ± 16 | 385 ± 5 | 3.6 ± 0.8 | 140 ± 1.0 | 25.6 ± 6.6 |
| SITE D | 124 ± 51 | 447 ± 23 | 0.6 ± 0.2 | 101 ± 1.5 | 185 ± 98 |

DOWNSTREAM INTENSIFICATION PATTERNS

By passing collimated 351nm CW light through each of the sites studied, an intensification pattern at various distances could be measured. Figures 5 and 6 show the intensification patterns at 2 and 120mm respectively. These patterns can be roughly characterized as having an on-axis “hotspot” component, present at both distances, and an off-axis “ring caustic” component present in all at short distances, but only for the largest undimpled site (Site C) studied at longer distances. These two components are also shown in Fig. 7, where we have indicated the relative focal distances for each. In the case of the on-axis component, the focal length Z_{OA} can be approximated using Fresnel optics as $Z_{OA} \sim 2r(a/h)$.

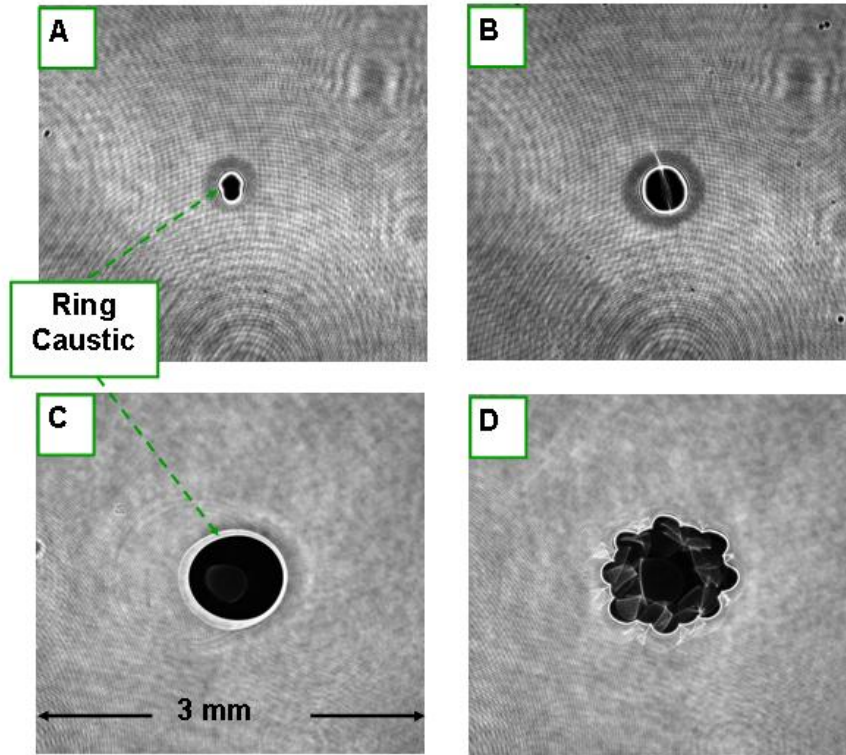


Figure 5: Intensification patterns at 2mm, showing an off-axis ring caustic.

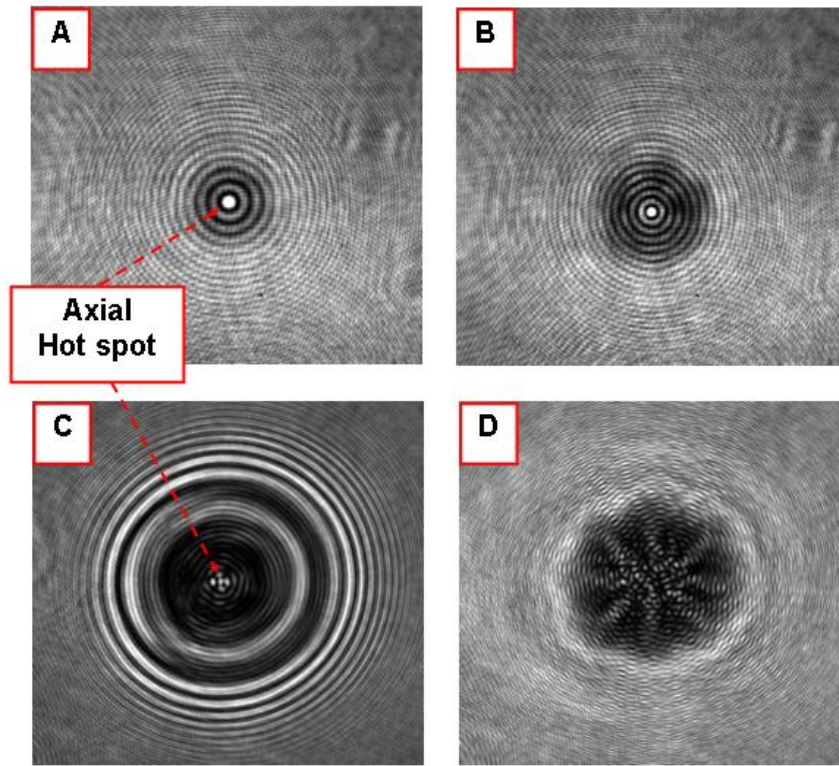


Figure 6: Intensification patterns at 120mm, showing an on-axis 'hotspot', and persistent off-axis ring caustic in the case of site C.

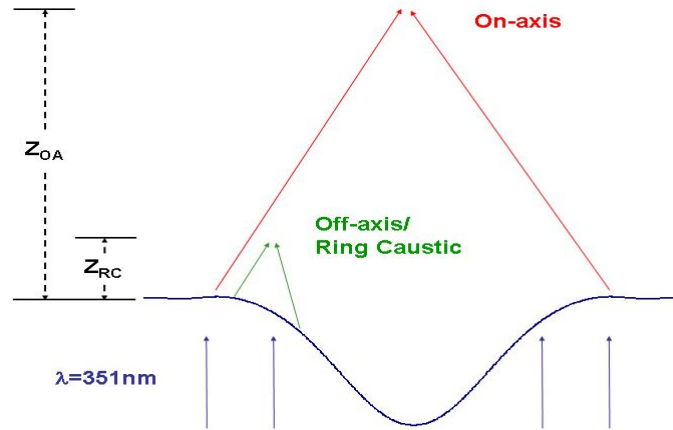


Figure 7: Relative positions of two dominant intensification patterns caused by axial symmetric exit surface depressions. Z_{OA} and Z_{RC} refer to the on-axis hotspot and off-axis ring caustic component focal lengths.

LASER INDUCED DAMAGE PREDICTIONS

Once the intensification pattern is known, given some background incident beam, the number of expected damage initiations is given by

$$\langle N \rangle = \int \rho[\phi(x, y)] dA \quad (1)$$

where $\rho(\phi)$ is the density of initiations at a given fluence and the integral is over the entire beam ($\phi \neq 0$). In order to illustrate the sensitivity of the damage initiations on the rim structure of the mitigation site, we calculate $\langle N \rangle$ for Sites C and D, both associated with large site mitigations, but one (Site D) that has been post-processed to modulate (“dimple”) the rim structure. As can be inferred from the intensification pattern shown above, Site C, with an intact rim structure is capable of high N values, while the rim-reduced Site D has N values less than 1 out to a distance of 150 mm. Figure 8 shows the dramatic difference between Sites C and D, where the effect of the rim structure on intensification is clear.

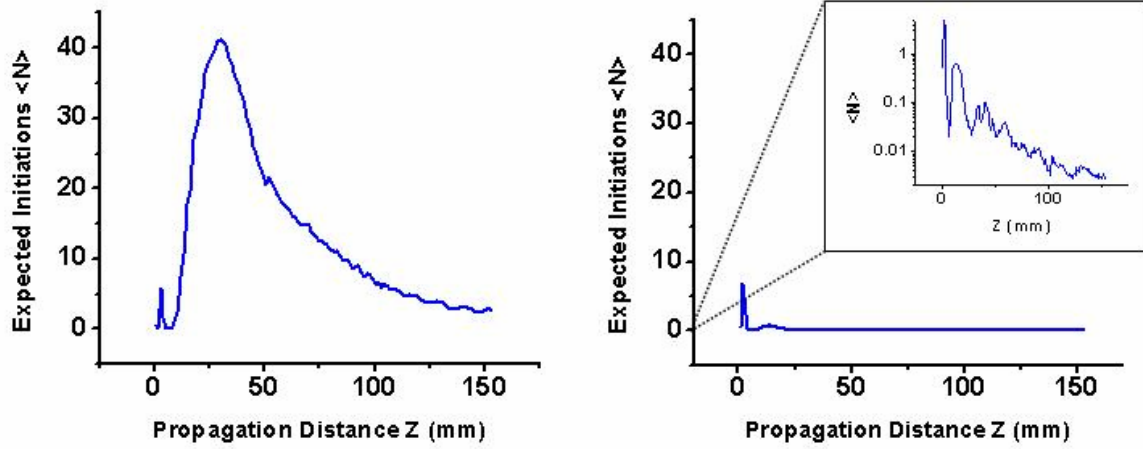


Figure 8: Calculation of the expected number of damage initiations for the undimpled (typical) site (Site C) and the dimpled (rim-reduced) site (Site D), showing a dramatic reduction in $\langle N \rangle$ for the latter case.

3 ω DAMAGE TESTING

Damage tests were conducted and results compared with predictions based on the intensification pattern and measured $\rho(\phi)$ for the samples studied. Figure 9 shows examples of the damage corresponding to on-axis and off-axis intensification of downstream light. The individual number of damage sites was counted for each site studied, and the results are shown in Table II.

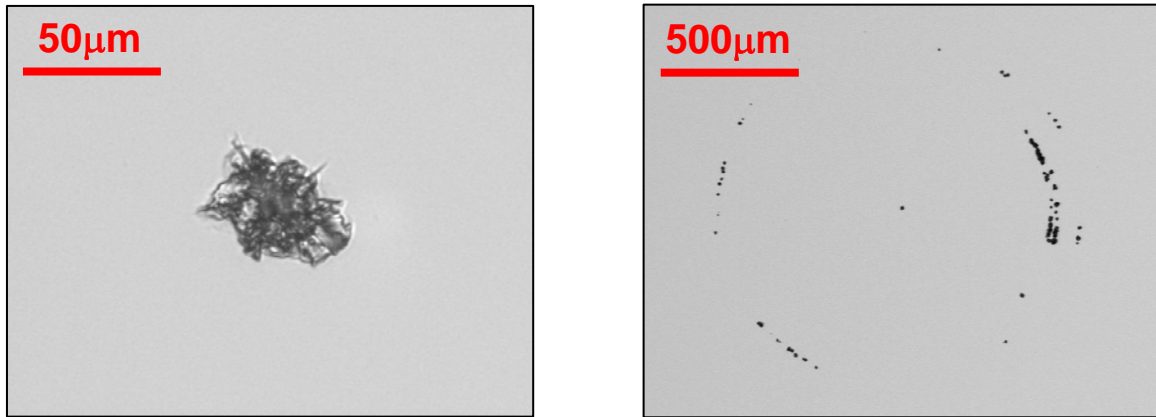


Figure 9: Damage caused on the exit surface of a fused silica optical sample located 120mm (opd) downstream from Site B (left) and site C (right), showing the result of on-axis and off-axis intensification respectively.

Table II: Results of damage testing fused silica optics located 120mm downstream from mitigation sites.

| Mitigation Site | Fluence at (J/cm ²) | Damage | <N> Calculated | N-Counted (# blobs) |
|-----------------|---------------------------------|--------|----------------|---------------------|
| SITE A | 7.0 | YES | 17 | 2 |
| SITE B | 6.5 | YES | 1.3 | 1 |
| SITE C | 5.1 | YES | 0.01 | 2 |
| SITE D | 4.3 | NO | $\sim 10^{-6}$ | 0 |
| SITE A | 7.6 | YES | 20 | 5 |
| SITE B | 8.5 | YES | 2.1 | 1 |
| SITE C | 8.8 | YES | 15 | >131 |
| SITE D | 7.6 | NO | 0.07 | 0 |

CONCLUSIONS

CO₂ laser exposures associated with the mitigation of fused silica damage result in a transformation of the damage site into an ablation pit and a surrounding rim structure that leads to downstream intensification which is characterized by on- and off-axis components. For small mitigation sites (A & B) with smaller rim structures ($r < 300\mu\text{m}$) off-axis components focused too fast to threaten downstream optics ($Z > 50\text{mm}$), whereas on-axis intensities tended to dominate over all distances studied ($< 150\text{mm}$). For the largest mitigation site where the rim structure remained intact (site C), both on-axis and off-axis components contributed to high downstream intensities, and, subsequently led to downstream optical damage. However, for the large dimpled-rim site (site D), the downstream intensification pattern is effectively dissipated preventing damage to downstream optics. The predicted number of damage sites and that observed scaled correctly, but differed in absolute quantity possibly due to counting errors in $\rho(\phi)$ estimates at high ϕ as well as hole drilling effects.

REFERENCES

1. R. R. Prasad, J. R. Bruere, J. Halpin, P. Lucero, S. Mills, M. Bernacil, R. P. Hackel, "Design of a production process to enhance optical performance of 3omega optics", [Conference Paper; Journal Paper] *SPIE-Int. Soc. Opt. Eng. Proceedings of the SPIE*, 5273 296 (2004)
2. I. L. Bass, G. M. Guss, R. P. Hackel, "Mitigation of laser damage growth in fused silica with a galvanometer-scanned CO₂ laser initiated surface damage in fused silica using a 4.6um wavelength laser" Conference Paper; Journal Paper] *SPIE-Int. Soc. Opt. Eng. Proceedings of the SPIE*, 5991 45 (2005)
3. G.M. Guss, "Mitigation of growth of laser initiated surface damage in fused silica using a 4.6 μm wavelength laser, [Conference Paper; Journal Paper] *SPIE-Int. Soc. Opt. Eng. Proceedings of the SPIE* 6403 6403-27 (2006)
4. E. Mendez, K. M. Nowak, H. J. Baker, F. J. Villarreal, and D. R. Hall, "The Localized CO₂ laser damage repair of fused silica optics" *Applied Optics*, Vol. 45, Issue 21, pp. 5358-5367 (2006)
5. M. A. Norton, E. E. Donohue, M. D. Feit, R. P. Hackel, W. G. Hollingsworth, A. M. Rubenchik and M. L. Spaeth, "Growth of laser damage in fused SiO₂ under multiple wavelength irradiation", [Conference Paper; Journal Paper] *SPIE-Int. Soc. Opt. Eng. Proceedings of the SPIE*, 5991 8 (2005)

6. I. L. Bass, V. G. Draggoo, G. M. Guss, R. P. Hackel, M. A. Norton, "Mitigation of laser damage growth in fused silica NIF optics with a galvanometer-scanned CO₂ laser," High-Power Laser Ablation VI, 6261-2A, *SPIE-Int. Soc. Opt. Eng. Proceedings of the SPIE*, 6261 45 (2006)
7. M. D. Feit, A. M. Rubenchik, C. D. Boley, M. Rotter, "Development of a process model for CO₂ laser mitigation of damage growth in fused silica" [Conference Paper; Journal Paper] *SPIE-Int. Soc. Opt. Eng. Proceedings of the SPIE*, 5273 145 (2004)